PHYSICAL REVIEW B **79**, 201201(R) (2009)

Unraveling the Jahn-Teller effect in Mn-doped GaN using the Heyd-Scuseria-Ernzerhof hybrid functional

A. Stroppa* and G. Kresse
Faculty of Physics, University of Vienna, Sensengasse 8/12, A-1090 Wien, AusCBMtria and Center for Computational Materials Science, Universität Wien, Sensengasse 8/12, A-1090 Wien, Austria
(Received 31 March 2009; published 1 May 2009)

We present an *ab-initio* study of the Mn substitution for Ga in GaN using the Heyd-Scuseria-Ernzerhof hybrid functional. Contrary to semilocal functionals, the majority Mn t_2 manifold splits into an occupied doublet and an unoccupied singlet well above the Fermi level resulting in an insulating ground state, which is further stabilized by a sizeable Jahn-Teller distortion. The predictions are confirmed using *GW* calculations and are in agreement with experiment. A transition from a localized to a delocalized Mn hole state is predicted from GaN to GaAs.

DOI: 10.1103/PhysRevB.79.201201 PACS number(s): 71.15.Mb, 71.20.Nr, 71.23.An, 71.55.−i

Semiconductor based spintronics aims to develop hybrid devices that could perform all three operations, logic, communications, and storage within the same materials technology.[1] Dilute magnetic semiconductors (DMSs) represent the most promising materials, and undoubtedly, transition-metal-doped III-V semiconductors are presently the workhorse for spintronics.[2]

Ab-initio simulations based on density-functional theory have played an important role in investigating the physics of DMSs.[3,4] Nevertheless, the theoretical understanding has been hindered by the well-known deficiencies of the spin-polarized local-density approximation (SLDA) and spin-polarized generalized gradient approximation (SGGA) to the exchange-correlation functional:[5] the nonlocality of the screened exchange interaction is not taken into account and the electrostatic self-interaction is not entirely compensated. This lack of compensation causes fairly large errors for localized states, e.g., the Mn *d* states. It destabilizes the orbitals and decreases their binding energy, leading to an overdelocalization of the charge density.[6] Another closely related issue is that the Kohn-Sham gap is usually a factor of 2–3 smaller than the fundamental gap of the solid.[5] Whenever the energy position of the defect level with respect to the valence-band maximum (VBM) is comparable with the Kohn-Sham gap, e.g., deep acceptor levels introduced by substitutional Mn in GaN (Mn_{Ga}),[7] the calculation of the thermodynamic transition levels becomes difficult since all predicted thermodynamic transition levels are strictly bound by the Kohn-Sham one electron gap. Although the underestimation of the one electron gap would even occur for the exact Kohn-Sham functional, discontinuities in the potential upon adding or removing electrons correct for this error.[5,8] For approximate functionals, which lack any such discontinuities—this includes all available semilocal and hybrid functionals—agreement between the Kohn-Sham gap and experimental fundamental gap is a prerequisite for modeling thermodynamic transition levels and band structure related properties.[5]

Hybrid Hartree-Fock density functionals[9] overcome the two limitations discussed above to a large extend.[5] Here, we apply the Heyd-Scuseria-Ernzerhof (HSE) hybrid functional[10] to study the Mn impurity in a GaN semiconductor host. Extensive studies of the performance of the HSE functional in solid-state systems can be found in Refs. 11–13, unequivocally showing that hybrid functionals outperform semilocal functionals for materials with band gaps. The HSE results are confirmed by GW_0 calculations, which are the benchmark method for the prediction of quasiparticle (QP) energies.[14] We will show that the electronic properties are accurately described by both methods. The t_2 manifold is split into an occupied doublet and an unoccupied singlet giving rise to a *symmetry-broken insulating* ground state that naturally couples with the ionic lattice, distorting the otherwise ideal tetrahedral environment of the Mn ion (Jahn-Teller effect). The calculated thermodynamic transition level $\epsilon(0/-)$ is in good agreement with experiments. Remarkably, most of these features are not captured by standard SLDA or SGGA, without introducing *ad hoc* corrections, such as self-interaction corrections[15,16] or LDA+*U* corrections.[17] Hybrid functionals have a single parameter (nonlocal exchange) that is once and forever fixed to 1/4 on theoretical grounds.[9] Furthermore, Stengel *et al.*[18] recently highlighted some drawbacks of SIC-schemes, concluding that hybrid functionals represent the most promising route to reduce self-interaction problems while preserving unitary invariance.

The calculations were performed using the projector augmented wave (PAW) method[19] with the Perdew-Burke-Ernzerhof (PBE) GGA functional[20] and HSE hybrid functional[10] recently implemented in the VASP code,[21] following exactly the prescription given in Ref. 22 (HSE06). The Ga 3*d* and Mn 3*p* electrons were considered as valence electrons. A soft nitrogen PAW potential was used, and the energy cutoff was set to 280 eV. Supercells with 64 and 128 atoms were used with lattice constants fixed to the optimized HSE value for the bulk crystal. Brillouin-zone integration was carried out using $8\times8\times8$ and $2\times2\times2$ Monkhorst-Pack grids for bulk GaN and the supercells, respectively. We used the Van der Walle and Neugebauer approach[23] for calculating the transition level of Mn_{Ga} using a 128 atom cell. For each charge state, the atomic positions were relaxed. Errors due to the electrostatic interactions were taken into account through the Madelung energy of point charges q in an effective medium with a static dielectric constant $\varepsilon_\infty=5.1$, $\Delta E_1=q^2\alpha/2\varepsilon_\infty L$, where L is the distance between

TABLE I. Lattice constant a, bulk modulus B_0, energy gap at Γ, L, X, dielectric constant ε_∞, valence-band width W, and the energy position of Ga d states determined using PBE, HSE, and GW_0. Spin-orbit splitting is not included ($\Delta_0 \approx 0.02$ eV). ε_∞ was calculated including local field effects and using the RPA (values in parentheses).

	PBE	HSE	GW_0	Expt.
a (Å)	4.546	4.494		4.506[a]
B_0 (GPa)	200	218		210
E_Γ (eV)	1.58	3.06	3.20	3.26[b]
E_L (eV)	4.49	6.18	6.32	
E_X (eV)	3.35	4.47	4.46	
ε_∞	5.86 (5.55)	5.1 (4.6)		≈5.3
W (eV)	7.1	7.9	7.4	6.7[c]
E_d	−13.3	−15.3	−15.7	−17.0 [d]

[a]Ref. 26.
[b]Refs. 27 and 28.
[c]Ref. 29.
[d]Ref. 30.

the Mn and its periodic replica and α is the Madelung constant.[24] ε_∞ was evaluated according to Ref. 13. For the GW_0 calculations, we determined the screening properties entering W_0 using the random-phase approximation (RPA) and PBE wave functions and eigenvalues but iterated the eigenvalues in G until self-consistency was reached. The initial wave functions and eigenvalues in G were determined using the HSE functional. For bulk materials, this procedure yields results that are within 5% of experiment and the self-consistent scGW procedure with vertex corrections that was used in Ref. 25. The latter procedure is out of reach for the systems considered here, but we expect the compromise to be very accurate since PBE yields good screening properties in the RPA and HSE excellent approximations for the true QP wave functions.[25]

In Table I we report the relevant equilibrium bulk parameters of GaN in the zinc-blende phase. The HSE lattice constant is very close to the experimental value at $T=0°$ K. The E_Γ^{HSE} band gap is 3.06 eV, almost twice as large as the PBE one (1.58 eV), again in very good agreement with experiment. Furthermore all HSE one-electron gaps are very close to the GW_0 QP energies. A slight discrepancy arises for the HSE valence-band width, for which PBE gives the best estimate (but experimental errors might be large). The position of the Ga d levels are described well using HSE, only surpassed by GW_0. Finally, the HSE dielectric constant agrees well with experiment. Overall, the agreement between experiment, HSE and GW_0 is very good.

Let us now consider the Mn substitution at the Ga host site. Figure 1 shows the band structure for the 64 atom cell plotted in the cubic Brillouin zone along the symmetry lines Δ and Σ. In the PBE band structure, the majority t_2 states form an essentially dispersionless impurity band pinned at the Fermi level. They are threefold degenerate at Γ with the partial occupancy of each state equal to 2/3. The three bands have predominantly t_2 character at the zone center (∼0.39), but they also show some antibonding contributions from the

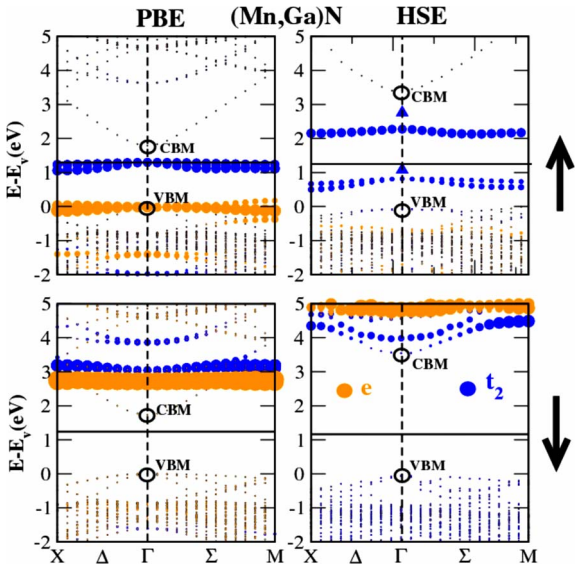

FIG. 1. (Color online) Spin-polarized projected band structure of the Mn impurity in a cubic 64 atom cell using PBE (left) and HSE (right). Majority (minority) bands are plotted in the upper (lower) part. The horizontal line corresponds to the Fermi level (energy zero is equivalent to valence-band maximum). The blue (dark gray) and orange (light gray) circles indicate the strength of the t_2 (i.e., $d_{xy}+d_{xz}+d_{yz}$) and e (i.e., $d_{x^2-y^2}+d_{3z^2-r^2}$) character, respectively. The VBM and CBM of the host crystal are shown by small empty circles. The majority doublet and singlet QP shifts are shown in the right part by blue triangles.

N-p states at the nearest N neighbors. The nonbonding e states can be found at the valence-band maximum, and they are strongly localized in the Mn sphere, with a total e character of ∼0.55. Below the e states, the GaN valence-band states are found. They are slightly hybridized with Mn states. For the minority component, the t_2 and e states are shifted above the host conduction band minimum (CBM) due to exchange splitting. The e states form a flat band even more localized than their majority counterpart (e character ∼0.80). The Fermi level is located in the gap in the minority component, while it cuts the t_2 bands in the majority states. Therefore, in the PBE description, $Mn_xGa_{1-x}N$ is a half metal for a Mn concentration of $x \sim 3.1\%$.

The HSE results differ significantly from the PBE results. First, the band-gap opening of the host is recognized. However, most relevant is that the majority t_2 states are *split* into an unoccupied singlet and an occupied doublet, which remains above the host VBM. The energy separation of the singlet and doublet is 1.46 eV at Γ, and the system is clearly insulating. The singlet state is strongly localized in the Mn sphere ($t_2 \sim 0.40$), whereas the doublet, which is close in energy to the valence band, is less well localized, with a d character of ∼0.20. The e states do not form a flat band anymore since they are pushed down in energy hybridizing more effectively with the host valence band. In the minority component, the t_2 band is not as flat as in the PBE case (see Fig. 1) but hybridizes more strongly with the first host conduction bands, especially at the zone boundaries, whereas the e states remain mostly unchanged, apart from a rigid upwards shift.

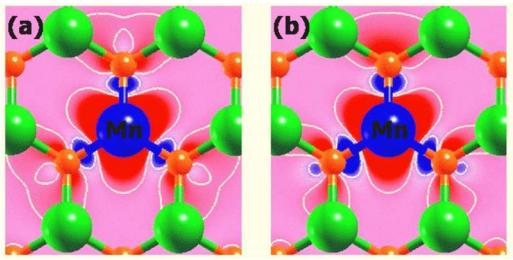

FIG. 2. (Color online) PBE (a) and HSE (b) spin-density contours between −0.03 and 0.02 $\mu_B/\text{Å}^3$ plotted on the (111) plane. Blue (dark gray) large spheres are Mn atoms; green (light gray) large spheres are Ga atoms; orange (light gray) small spheres are N atoms. Red (dark gray) and blue (light gray) regions correspond to positive and negative spin-density. Note the lack of the C_3 symmetry in (b).

Remarkably, we observe that the quasiparticle GW_0 band structure is essentially identical to the HSE one-electron energies. In the GW_0 calculations, the doublet and the singlet shift upwards away from the VBM by 0.25 and 0.43 eV compared to the HSE case, but the energy separation remains almost unchanged. This suggests that HSE is a legitimate shortcut for sophisticated many electron calculations, an observation that already transpires from the very good HSE one-electron band gaps. The GW_0 calculations also clearly confirm that the metallic state observed in DFT-PBE is an artifact of the involved approximations. In fact, a band gap can be predicted using DFT-PBE as well, if (and only if) the band gap is calculated as the energy difference between the ionization potential and electron affinity calculated by removing and adding *one* electron in *one* supercell (~1 eV). However, if a single electron or hole were placed in a huge supercell with many Mn substitutional sites, DFT-PBE would predict the electron affinity and ionization potential to be equal (metal), whereas the hybrid functional would predict the band gap even in the limit of low electron or hole concentrations. The latter result is correct, whereas the PBE result is not in agreement with experiment.[31]

Another visible consequence of the splitting of the t_2 states is the Jahn-Teller distortion around the defect. The Mn t_2 states do not transform as an irreducible representation of the T_d group since they are not threefold degenerate. This effect is usually termed "spatial symmetry breaking."[32] The splitting is even obtained at the *ideal* ionic structure, and for the ideal structure, three equivalent electronic solutions with identical energies are found. Each of the electronic solutions corresponds to a different orbital ordering, and once the lattice is allowed to relax the nuclear framework distorts accordingly, i.e., the Jahn-Teller effect is at play.

Figure 2 shows the spin density around the Mn atom in the (111) plane in the ideal structure, for both (a) PBE and (b) HSE calculated for a 128 atom cell, sampling the Brillouin zone at the Γ point only. The PBE spin density is clearly symmetric, while in the HSE case the symmetry is spontaneously broken with the C_3 symmetry around all {111} directions missing. We can determine the subgroup associated with the Jahn-Teller distortion by considering the character tables of all the possible subgroups of T_d (Ref. 33) and

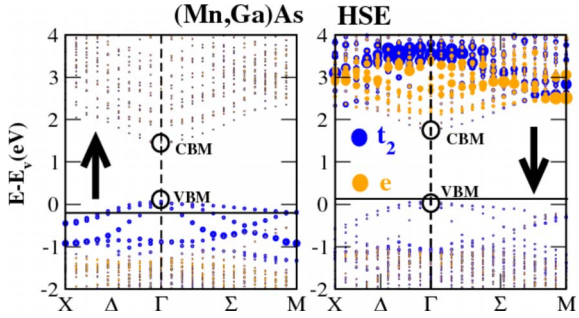

FIG. 3. (Color online) HSE spin-polarized projected band structure of the Mn impurity in a cubic GaAs 64 atom cell. See caption Fig. 1 for details.

taking into account that (i) the t_2 manifold is split into a singlet and a doublet and (ii) that the subgroup must not contain the C_3 symmetry operation. The only subgroup compatible with (i) and (ii) is D_{2d}. By allowing the ions to relax without symmetry constraints, it is found that the tetrahedral environment around the Mn atom becomes distorted: two of the Mn-N bonds relax to 1.98 Å, while the other two bonds relax to 1.97 Å (the ideal GaN distance is 1.94 Å). The relaxed structure is within numerical uncertainty indeed consistent with the D_{2d} symmetry, in agreement with experiments.[34] The energy gain due to relaxations is 184 meV/Mn. Semilocal functionals (PBE) are not able to capture the Jahn-Teller distortion *unless* one introduces *ad hoc* symmetry-breaking displacements but even then the energy gain due to the symmetry breaking is certainly significantly underestimated.[35]

As a final confirmation of the HSE results, we have calculated the $\epsilon(0/-)$ thermodynamic transition level for Mn_{Ga} in GaN by adding an electron in the HSE calculations and relaxing the geometry. We obtained a value of 1.9 eV comparing notably better with experiment [1.8 ± 0.2 eV (Ref. 36)] than PBE calculations (1.6 eV). In order to test the predictive capability of the procedure, we have repeated the calculations for Mn_{Ga} in GaAs, for which Mn is experimentally found in a d^5 configuration.[35] In this case, the splitting of the t_2 states drops to ~0.2 eV, and no Jahn-Teller effect is theoretically found using HSE or experimentally expected.[35] Furthermore, the HSE band structure for Mn in GaAs (Fig. 3) shows that HSE predicts a metallic behavior for the majority electrons. Hence the hole introduced by Mn shows a transition from a *localized* to a *delocalized* character from GaN to GaAs, in full accordance with all experimentally available data.

A further confirmation of the accuracy of the present approach is that it is capable to predict the position of the Mn *d* states, which are found at an average binding energy of 4.2 eV in photoemission experiments for GaAs,[37] in very good agreement with the HSE results, while in SLDA or SGGA, the spectral weight is shifted toward the Fermi level.

In summary, we have shown that the HSE functional predicts the localization of one electron hole at the Mn impurity in GaN giving rise to a Jahn-Teller distortion and an insulating ground state via splitting of the t_2 Mn manifold. The existence of a band gap was confirmed by GW_0 quasiparticle calculations and is in agreement with experiment. The for-

malism is able to predict the relevant electronic features without imposing *ad hoc* corrections on the *d* states and includes ionic relaxations. Furthermore, a change in the electronic hole state from a localized character in GaN to an itinerant band in GaAs is predicted. This observation agrees with the fact that the localization is strongly environment dependent.[18] Previous interpretations of optical experiments[38] based on standard DFT electronic structure calculations should be revised according to the picture emerging in this Rapid Communication. Likewise, magnetic interactions should be reinvestigated using functionals that predict a band gap in the quasiparticle spectrum. Extension to IV-group DMS[39] are currently in progress.[40]

This work was supported by the Austrian Fonds zur Förderung der wissenschaftlichen Forschung. A.S. thanks K. Hummer for technical assistance in the calculation of dielectric properties.

*Presently at CASTI Regional Laboratory, Consiglio Nazionale delle Ricerche, Istituto Nazionale di Fisica della Materia (CNR-INFM), 67100 L'Aquila, Italy. Email: astroppa@aquila.infn.it

[1] D. D. Awschalom and M. E. Flatté, Nat. Phys. **3**, 153 (2007).
[2] I. Žutić, J. Fabian, and S. Das Sarma, Rev. Mod. Phys. **76**, 323 (2004).
[3] J. Kudrnovský, I. Turek, V. Drchal, F. Máca, P. Weinberger, and P. Bruno, Phys. Rev. B **69**, 115208 (2004).
[4] P. Mahadevan and A. Zunger, Phys. Rev. B **69**, 115211 (2004).
[5] S. Kümmel and L. Kronik, Rev. Mod. Phys. **80**, 3 (2008).
[6] T. C. Schulthess, W. M. Temmerman, Z. Szotek, W. H. Butler, and G. M. Stocks, Nature Mater. **4**, 838 (2005).
[7] P. Mahadevan and A. Zunger, Appl. Phys. Lett. **85**, 2860 (2004).
[8] B. J. Janesko, T. M. Henderson, and G. E. Scuseria, Phys. Chem. Chem. Phys. **11**, 443 (2009).
[9] A. D. Becke, J. Chem. Phys. **98**, 1372 (1993); J. P. Perdew, M. Ernzerhof, and K. Burke, *ibid.* **105**, 9982 (1996).
[10] J. Heyd, G. E. Scuseria, and M. Ernzerhof, J. Chem. Phys. **118**, 8207 (2003); **124**, 219906(E) (2006).
[11] J. Heyd, J. E. Peralta, G. E. Scuseria, and R. L. Martin, J. Chem. Phys. **123**, 174101 (2005).
[12] J. Paier, R. Hirschl, M. Marsman, and G. Kresse, J. Chem. Phys. **122**, 234102 (2005) J. Paier, M. Marsman, K. Hummer, G. Kresse, I. C. Gerber, and J. G. Ángyán, *ibid.* **124**, 154709 (2006); J. Paier, M. Marsman, and G. Kresse, *ibid.* **127**, 024103 (2007); M. Marsman, J. Paier, A. Stroppa, and G. Kresse, J. Phys.: Condens. Matter **20**, 064201 (2008); A. Stroppa and G. Kresse, New J. Phys. **10**, 063020 (2008).
[13] J. Paier, M. Marsman, and G. Kresse, Phys. Rev. B **78**, 121201(R) (2008).
[14] L. Hedin, Phys. Rev. **139**, A796 (1965).
[15] J. P. Perdew and A. Zunger, Phys. Rev. B **23**, 5048 (1981).
[16] A. Filippetti and N. A. Spaldin, Phys. Rev. B **67**, 125109 (2003).
[17] V. I. Anisimov, F. Aryasetiawan, and A. I. Liechtenstein, J. Phys.: Condens. Matter **9**, 767 (1997).
[18] M. Stengel and N. A. Spaldin, Phys. Rev. B **77**, 155106 (2008).
[19] P. E. Blöchl, Phys. Rev. B **50**, 17953 (1994).
[20] J. P. Perdew, K. Burke, and M. Ernzerhof, Phys. Rev. Lett. **77**, 3865 (1996).
[21] G. Kresse and J. Furthmüller, Phys. Rev. B **54**, 11169 (1996).
[22] A. V. Krukau, O. A. Vydrov, A. F. Izmaylov, and G. E. Scuseria, J. Chem. Phys. **125**, 224106 (2006).
[23] C. G. Van de Walle and J. Neugebauer, J. Appl. Phys. **95**, 3851 (2004).
[24] M. Leslie and M. J. Gillan, J. Phys. C **18**, 973 (1985).
[25] M. Shishkin, M. Marsman, and G. Kresse, Phys. Rev. Lett. **99**, 246403 (2007).
[26] F. Benkabou, H. Aourag, P. J. Becker, and M. Certier, Phys. Status Solidi B **209**, 223 (1998).
[27] http://www.ioffe.ru/SVA/NSM/Semicond/
[28] I. Vurgaftman, J. R. Meyer, and L. R. Ram-Mohan, J. Appl. Phys. **89**, 5815 (2001).
[29] T. Maruyama, Y. Miyajima, K. Hata, S. H. Cho, K. Akimoto, H. Okumura, S. Yoshida, and H. Kato, J. Electron. Mater. **27**, 200 (1998).
[30] G. Martin, A. Botchkarev, A. Rockett, and H. Morkoc, Appl. Phys. Lett. **68**, 2541 (1996).
[31] G. M. Dalpian and S.-H. Wei, Phys. Rev. Lett. **93**, 216401 (2004).
[32] N. J. Russ, T. D. Crawford, and G. S. Tschumper, J. Chem. Phys. **120**, 7298 (2004).
[33] http://www.cryst.ehu.es/ and http://www.webqc.org/symmetry.php
[34] A. Wolos, A. Wysmolek, M. Kaminska, A. Twardowski, M. Bockowski, I. Grzegory, S. Porowski, and M. Potemski, Phys. Rev. B **70**, 245202 (2004).
[35] X. Luo and R. M. Martin, Phys. Rev. B **72**, 035212 (2005).
[36] T. Graf, M. Gjukic, L. Görgens, O. Ambacher, M. S. Brandt, M. Stutzmann, J. Supercond. **16**, 83 (2003).
[37] J. Okabayashi, A. Kimura, T. Mizokawa, A. Fujimori, T. Hayashi, and M. Tanaka, Phys. Rev. B **59**, R2486 (1999).
[38] J. Zenneck, T. Niermann, D. Mai, M. Roever, M. Kocan, J. Malindretos, M. Seibt, A. Rizzi, N. Kaluza, and H. Hardtdegen, J. Appl. Phys. **101**, 063504 (2007).
[39] A. Stroppa, S. Picozzi, A. Continenza, and A. J. Freeman, Phys. Rev. B **68**, 155203 (2003).
[40] A. Stroppa, G. Kresse, and A. Continenza (unpublished).